Active Control of Wind Turbine Blades to Increase Efficiency

A Technical Paper submitted to the Department of
Mechanical & Aerospace Engineering University of Virginia
MAE 4620: Machine Design II

Written By:

Jason Badu

Charles Breen

Charles Breen

Astrid Henkle

Amanda Kassebaum

Amanda Kassebaum

Scott Morrow

Isaiah Woo

Isaiah Woo

Approved M E Momot Date 12/15/2021

ADVISOR: Michael Momot, Department of Mechanical & Aerospace Engineering

December 14, 2021

Introduction

As environmental conditions around the globe have worsened over the past couple decades, governments have started to prioritize the fight against climate change with the use of new renewable energy technology. The shift has been particularly noticeable in the United States, where consumption of renewable energy has already risen to 21% of total electricity generated in 2020, a number that continues to grow steadily each year (EIA, 2021). The fastest growing and most widely used renewable resource is wind energy, which accounted for 42.7% of renewables in 2020 (UMCSS, 2021). With a relatively new yet rapidly growing industry, it is important to find ways of improving the technology quickly as global climate change concerns necessitate an effective solution to rising global temperatures.

The increasing prevalence of wind energy has resulted in a glaring problem: the limited maximum efficiency of the technology. Power generated by a wind turbine is linearly correlated to the swept area of its blade, and manufacturers have shown that by simply increasing the length of each blade and the height that a turbine hub sits, efficiency is increased and so is total energy output (energy.gov, 2021). Engineers have concentrated on increasing blade length because the equation that describes how a wind turbine produces power, known as the power generation formula, shows that power is proportional to the swept area. The equation is as follows where P is power, C_p is the coefficient of performance (which is the amount of available wind energy used by the wind turbine out of the total amount of wind energy available), ρ is air density, V is air speed, and A is area swept by the turbine blade:

$$P = C_p \rho V^3 A \quad (1)$$

Turbine blades cannot keep increasing in length, as manufacturing, geographical, and

space limitations dictate that other solutions for increased efficiency must be developed. A less common approach is to actively change the blade shape to improve C_p, which will be explored in this project.

This limitation of the maximum C_p, known as the Betz limit, must be addressed as limitations are beginning to hinder the growth of development in the industry. Developing another successful method to increase energy production efficiency is crucial to continue the implementation of wind energy. Therefore, this project's mission is to increase the efficiency of wind turbines by using active control systems to increase power production at lower wind speeds between the cut-in speed and peak power production speed. The efficiency of the improved wind turbine will then be compared to the known performance data of real-life wind turbines to compare results.

Background

Current Technology

In the wind turbine industry today, there are multiple methods being employed to increase efficiency of the technology. As discussed in the introduction, the simplest way to accomplish a greater energy efficiency is to increase the size of the wind turbines. The size of wind turbines has grown significantly over the past three decades, and so has the average rated power for each model, as shown in Figure 1.

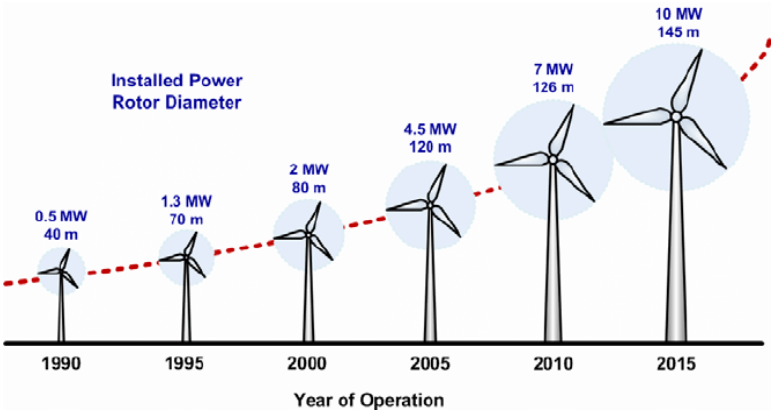

Figure 1: Size evolution of wind turbines over time (ResearchGate, n.d.)

This method has proved to be successful up until this point in the industry's history, as size has now become a constraint. With manufacturing blades hundreds of meters long, transportation is nearly impossible, especially on roads that aren't easily accessible. A proven solution to increasing wind turbine efficiency over time also has limitations that are already being reached by the industry.

Another common form of increasing a turbine's energy output is through a method known as pitch control. Pitch control adjusts the angle of attack of the blades to ensure that the proper ratio of available wind energy is being utilized by the wind turbine (Opie, 2018). The purpose of this technology is directed towards the protection of the turbine exceeding its maximum rotational speed in the case of extreme winds to prevent damage to the machine or the electrical grid. Rather than increasing the efficiency of a turbine, this method of blade adjustment is geared towards protection of the technology and has been utilized on most modern devices.

One method of passively increasing the efficiency in the blades is the addition of tubercles on the leading edge of a blade. Inspired by the structure of a humpback whale's flipper, testing has shown that the turbulent flow that is created by these serrations in a wind turbine

blade can actually reduce noise, increase stability, and allow more energy to be captured by a turbine from the wind (Hamilton, 2008). Figure 2 displays the tubercles on a wind turbine blade. While this passive method of improving wind turbine blade efficiency is effective, the lack of active control over the technology does not permit for the most efficient utilization of the available wind at all speeds, but rather just marginally increases the efficiency altogether.

Figure 2: Tubercles on leading edge of wind turbine blade (Hamilton, 2008)

Constraints

Before fully developing a design for the experiment, multiple constraints were considered to prepare for the possible challenges that would be encountered over the course of the project. The main constraints that affected the group's work were cost, schedule, constructability, manufacturability, and scalability. These constraints were broken up into groups to identify a successful path for the project's design and implementation.

The main issues to consider were cost and schedule. Knowing that the group had an expense limit set at $666 and about four months to complete the overall experiment, a rigid timeline and spending plan was developed. If an official company worked on the project, the budget and time frame to accomplish the main goal is expected to be significantly larger and longer, so the objective of the group was to find a cheap way to construct the final design and

manage to find results as quickly as possible to develop a connection to a real world wind turbine. Despite difficulties extrapolating materials used in this scenario and scalability concerns, the goal was to design and validate a new method to improve the wind turbine efficiency to provide real world companies with a possible solution to efficiency issues.

The remaining constraints of the experiment were constructability, manufacturability, and scalability. The wind tunnel that was available for testing only had a one cubic foot testing space inside the device, so any turbine created had to go behind the tunnel and fit within a space measuring around 4 ft in diameter. Therefore, constructability was also a problem as the designed mechanism had to fit in the very limited space inside the blades and tolerancing was very tight. Since this experiment was being conducted under an aggressive scalability constraint that presented many unknown challenges to the group, the issue of manufacturability also had to be addressed. On a full scale, the development of the active control system and blades for the turbine of the project would be completely different, therefore a direct connection between the experiment's results of a smaller turbine cannot be made without further research on a larger scale.

Specifications

Aside from improving the efficiency and power output of the turbine, specifications require that the turbine design remain durable in the presence of high winds. Typical wind turbine blades themselves must be able to withstand spinning at speeds of more than a hundred miles per hour at their tips. While it is necessary on some occasions, shutting down and locking up turbines due to intense winds is not desirable. Furthermore, specifications made clear that the cost of any design be taken into account. Costs accounting for materials, labor, and maintenance were essential to acknowledge as they heavily affect the competitiveness of any design in the

wind turbine market. In short, an effective design is not useful in industry if it is more expensive than alternative options. A failure mode & effects analysis (FMEA) and levelized cost of energy (LCoE) will be performed to evaluate the reliability and cost performance of the designed turbine.

Design Process

Concept Selection and Decision Making

After establishing the overall goals for the project, each team member came up with 2-3 ideas to address the challenges. The team then created criteria which was used to judge each concept. The screening and scoring criteria included constructability, energy use, reliability, scalability, weight, energy production, and precision of movement. The team collectively screened 10 concepts against this criteria and selected 4 concepts to continue to the next step of the concept selection process, one concept being a combination of two prior concepts from the screening process (Appendices A-1 and A-2, Figures 3-6).

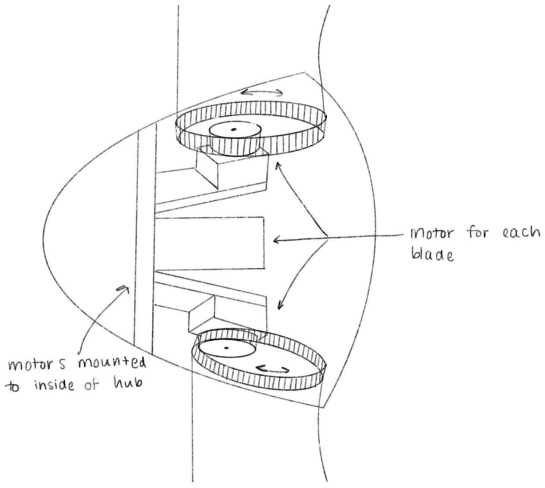

Figure 3: Concept A - Pitch Control with 3 Separate Motors

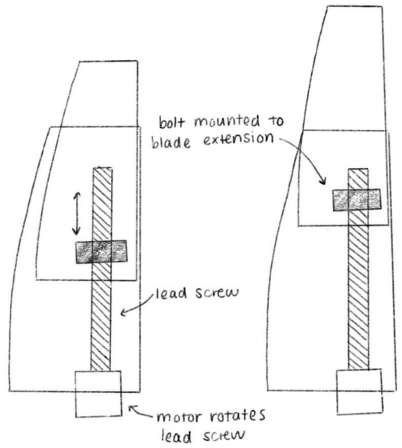

Figure 4: Concept B/I - Motor and Lead Screw to Extend Blade Length

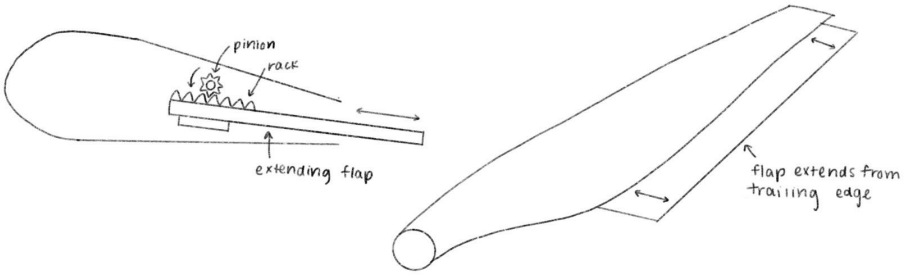

Figure 5: Concept D - Rack and Pinion to Extend Blade Width

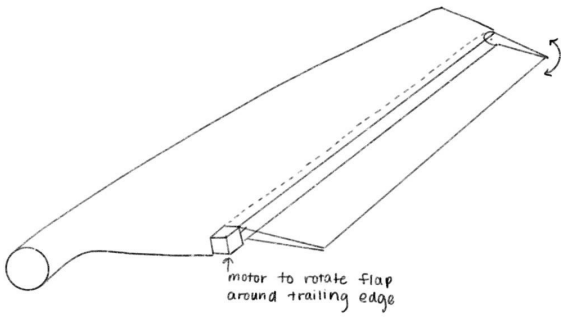

Figure 6: Concept F - Airplane Flaps with Motor

The scoring matrices in Appendix A-2 resulted in all four concepts having competitive scores which required the use of intuition and mechanical knowledge to select between the similarly rated concepts. Concept F scored the lowest, and while this design has increased lift forces on airplane flaps, it was not selected due to constructability concerns as the blade would be small and it would be difficult integrating a motor on the trailing edge of the blade. Due to size constraints, it would be more optimal to have a motor located in a thicker part of the blade or inside the hub. Concept B/I would be efficient in increasing the power production of the wind turbine as it increases the length, and therefore the swept area of the blade. This increased swept area allows the turbine to collect more energy from the wind and produce more power at lower speeds. Creating larger blades is already an idea that is instituted in industry; however, the size of the blade is restricted due to transportation issues. Concept B/I would solve this problem due to its ability to extend and retract. Overall, this concept is more relevant to the current goal of modularity in the wind turbine industry, as dictated by Apex Clean Energy, a local wind energy company in Charlottesville, VA. Another limitation to increasing the length of the blade is that as the length of the blade increases, the tangential velocity at the tip of the blade increases. This is according to Equation 2 where v is the tangential speed, r is the distance from the center of the hub, and ω is the angular velocity of the turbine. This increased velocity results in larger centripetal forces as seen in Equation 3, where F_r is centripetal force and m is mass. Figure 7 shows a free body diagram of the centripetal forces which could damage the wind turbine blades as the length of the blades increase. This concept would also be too big to test behind the available wind tunnel. For these reasons, along with constructability concerns, concept B/I was not selected.

$$v = r\omega \quad (2)$$

$$F_r = \frac{mv^2}{r} \quad (3)$$

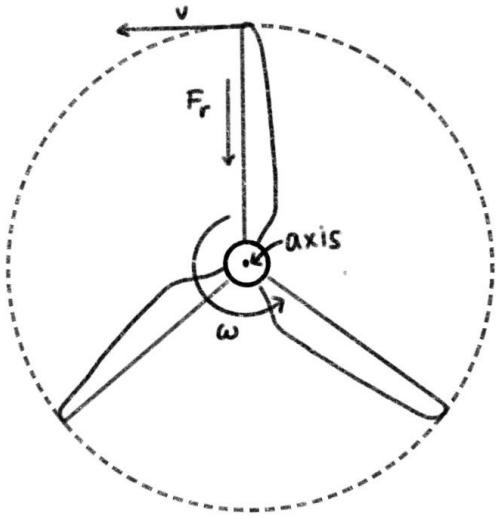

Figure 7: FBD of Centripetal Forces Acting on the Wind Turbine

Regarding concept A, pitch control is already widely used in industry to increase the power production of wind turbines by actively adjusting the angle of attack of the wind turbine blades. Since this concept has already been implemented in industry, it was not selected for this project. Concept A would also be difficult in terms of scalability since it would be difficult to fit these mechanisms in a turbine small enough to fit behind the available wind tunnel. Finally, the team decided to select concept D which involved extending a flap from the trailing edge of the blade using a rack and pinion driven by a motor. The aim of this concept is to delay the separation of the boundary layer which results in a larger wake and would allow the turbine to capture more energy from the wind and increase the coefficient of performance, C_p. Concept D also did not have any major concerns regarding the screening and scoring criteria and scored the highest. While the goal of Concept D was considered the best, there were concerns that the rack and pinion movement method would be too large to fit within the blade. For that reason,

additional movement methods were considered. The goal of the mechanism was to reliably extend and retract a thin flap from the blade without significantly disrupting the aerodynamics of the blade profile. With this goal in mind, two new methods of movement were thoroughly considered.

The first method of movement was using a four-bar mechanism, with the motor powering the mechanism being located in the hub of the turbine, and the four-bar's axles running along the length of the blade. The basic idea for this mechanism is shown below in Figure 8.

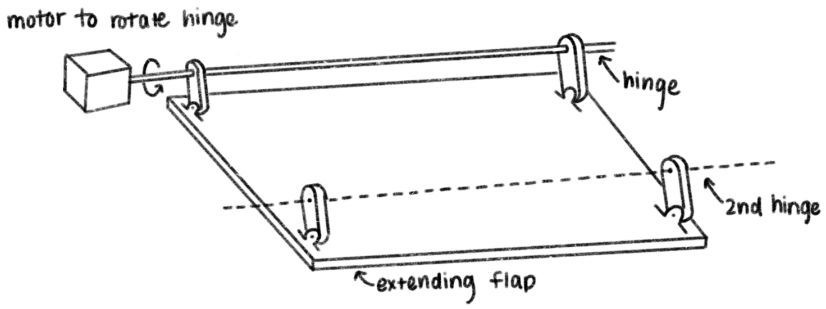

Figure 8: Four-Bar Mechanism for Flap Extension

This mechanism would only have two positions for the flap: retracted and extended. The retracted position would have the flap resting against the bottom surface of the blade, adding no area to the blade and mimicking a blade with no mechanism. The extended position would be where the four-bar has rotated to move the flap, and the flap remains partially resting on the four-bar, with the remainder of the flap extending out beyond the trailing edge of the blade. This option offers the advantage of reliability, as the four-bar is well constrained in its range of motion. There were several issues with this concept given the other design constraints. In particular, the four-bar linkages would have to be very tightly toleranced and located at such a

small scale, making it difficult to manufacture. Additionally, this mechanism would dramatically disrupt the air flow around the blades while transitioning between the retracted and extended positions. After considering these weaknesses, the concept was rejected for the second method of movement.

The second method involved using springs to push the flap out of the wing to some maximum extended position. The flap would be attached by string to a motor located in the hub, which would then rotate and wrap the string around its axle to retract the flap. The full mechanism concept is found below in Figure 9.

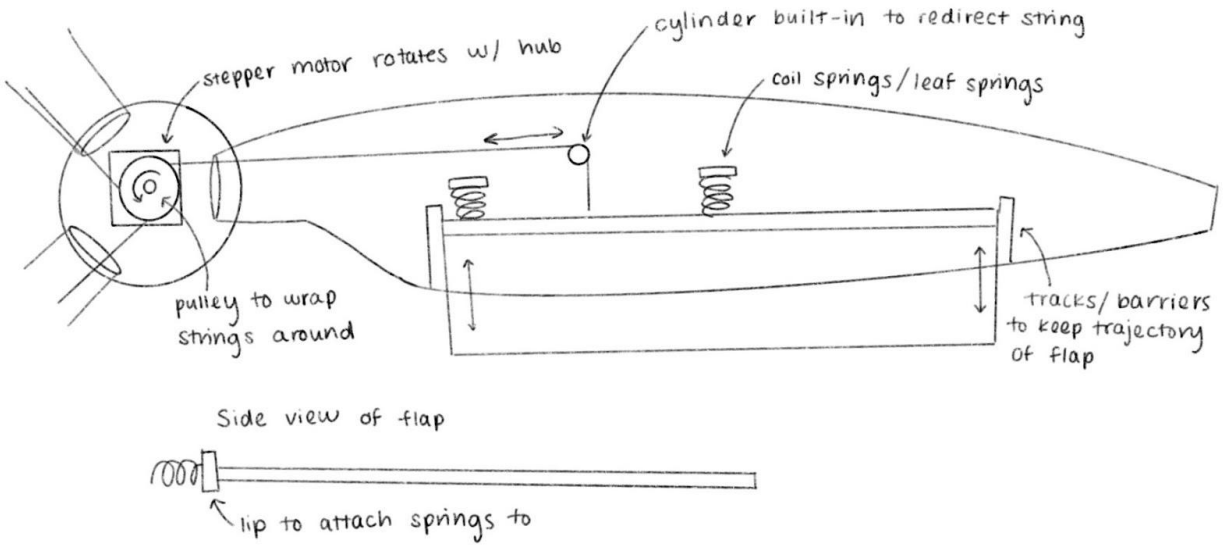

Figure 9: Original Spring-String Mechanism Design

This concept offered several advantages over the four-bar. For one, the largest component, the motor, could be located in the hub where there is much more space when compared to the blades. There's also no moving joints with this mechanism, allowing for slightly looser tolerances. The springs and strings are also very small and could therefore feasibly be located entirely within the blade, minimizing aerodynamic disruption. Additionally, the motor position could be adjusted to configure what length of flap is extended, as opposed to the

four-bar which could only be extracted or retracted. This mechanism was also chosen over the rack and pinion mechanism in concept D from the concept selection process because it is much lighter than a rack and pinion and would be easier to fit in the limited space inside the blade. With these advantages in mind, the spring-string mechanism was selected over the four-bar after moving forward from the original idea of the rack and pinion system.

Prototyping:

With a detailed design concept completed, the next step was to prototype a mechanism. The first prototype, pictured below in Figure 10, was simply to test the basic functionality of the spring-string mechanism and discover any possible problems with the mechanism that should be anticipated for future iterations of the design.

Figure 10: First Prototype of Spring-String Mechanism

This prototype revealed that more formal spring calculations would be critical to ensure sufficient flap movement. These calculations would be necessary to determine the smallest possible motor that would be strong enough to resist the force of the springs in all three blades. Another consideration was where the natural frequency of the spring-flap system would be, and whether the rotation of the blades might cause undesired vibrations. It also revealed that

whatever motor was selected would have to be fairly precise and have sufficient holding power at a given torque.

CFD:

In parallel to designing and prototyping the mechanism, computational fluid dynamics (CFD) simulations were performed to validate the broader design concept. To do this, a wind turbine blade was modeled using the NACA 4421 design from the NACA airfoil database (NACA, n.d.). This particular airfoil had features characteristic of a typical full size air turbine blade, making it suitable for simulation purposes. The blade model was scaled to be 22 inches long, which would later be the actual print length. A hollow slot for the flap to retract into was added to the back end of the blade, and CFD simulations were performed with the flap at varying degrees of extension. A wind speed of 50 mph, or 880 in/s, was selected for the simulations. To recreate the effects of an angle of attack of 15 degrees, the wind speed in the x-direction, parallel to the blade, was set to 880cos(15), while in the y-direction, perpendicular to the blade, was set to 880sin(15). The global mesh size was set to 4 for all trials, and the cut plots were located in the same place for all runs. A surface goal consisting of the net force in the y-direction was created to represent the lift force exerted on the blade. The resultant lift forces and cut plots are summarized in Figures 11 and 12 respectively.

No Flap	.843 lbf

Extended Flap	
Length (in)	Lift (lbf)
0.75	1.364
1	1.677
1.25	1.422

Figure 11: Lift Force Values

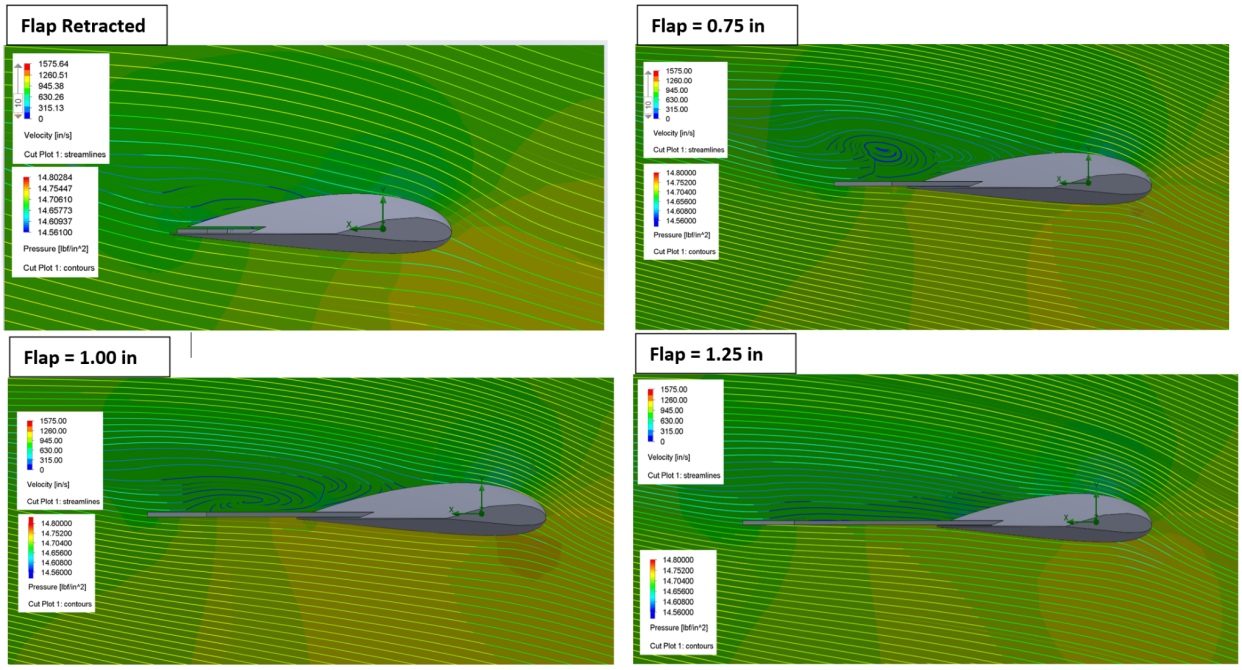

Figure 12: CFD Cut Plots

These results reveal two important pieces of information. The first is that the addition of the flap, at least in these conditions, does increase the lift. The lift force is notably higher for each test with flap extension versus that with the flap fully retracted. The second is that this effect does begin to diminish and actually decrease the lift beyond a certain flap length. In this case it occurs somewhere between a flap length of 1 in and 1.25 in. These results indicate that the addition of the extending flap mechanism should increase lift (and therefore power production) at some wind speeds, but also to not make the flaps too long or else the effect will actually start to decrease lift.

Spring Selection:

The goal of the spring selection process was to identify the smallest springs possible that would offer sufficient resistance and deflection while also avoiding the system's natural frequency. The largest factor driving the spring size was the size of the blade. The blade size was limited to just under 2 feet, given the limited size of the wind tunnel exit that would be used for

testing. With this in mind, the turbine blade model was scaled accordingly, and the thickness of the blade became the limiting factor of the spring size. It was in this way that a spring outer diameter of .088" was selected. Again, the blade dimensions also played a significant role in determining the maximum free length of the spring, leading to a selection of 0.56". With these two dimensions decided, the spring rate is limited to whatever the manufacturer is making in those dimensions. In this case, one spring was a valid candidate, and its statistics are summarized below in the blue cells of Figure 13. Relevant calculations were then made using these values, found in the white cells. The formula for maximum spring force is as follows where k is the spring rate, and x is the maximum deflection of the spring :

$$F = kx \tag{4}$$

The net force exerted by springs in parallel is simply the sum of the spring forces. Therefore for 2 springs in parallel, the net force is two times F, and for all blades, it is 6 times F.

k (lb/in)	Free Length (in)	Solid Length (in)	δ (in)	F (lb)
1.045	0.56	0.112	0.394	0.41

# in ||	F (lb)	For all blades (lb)
2	0.82	2.47038

Figure 13: Selected Spring Characteristics

These statistics indicate that the motor in the hub needs to only be strong enough to resist about 2.47 lbs about its axle in order to fully compress all six springs and thus fully retract the flaps. Another consideration made regarding the spring was the natural frequency of the spring-flap system. Given the spring constant of 1.045 lb/in and an average flap mass of 2.3 g, the natural frequency can be found using the following formula where $\boldsymbol{\omega}_n$ is the natural frequency, k is the spring constant, and m is mass:

$$\boldsymbol{\omega}_n = \sqrt{\frac{k}{m}} \quad (5)$$

The resulting natural frequency of the entire system, including all six springs and all three flaps, is 12.63 rad/sec. The risk of vibration damage at this frequency was deemed insignificant, given the precision of the angular velocity needed to trigger such an event, and the unlikeliness of the wind speed ever being held at that specific value for any extended period of time.

3D Modeling:

The initial blade design was established as described in the CFD process description, although the initial blade was scaled to a length of 10 in. This blade was printed in portions and and the parts were fixed together using JB weld epoxy. This initial print showed the model was of sufficient quality, and also exposed the challenge of reliably aligning the blade pieces. To address this, interlocking tabs and slots were added to the parts so they could be aligned and epoxied together.

The next model was larger, with the blade now scaled to 22 inches in length. It contained the first physical iteration of the mechanism, and was printed in five pieces, with the portion containing the mechanism split down the middle parallel to the blade. This iteration revealed more issues. For one, the print orientation was incorrect, resulting in a rough surface finish and weaker structure. Additionally, some minor physical issues with the mechanism design were exposed, that were then adjusted in the 3D model for the following iteration.

The final blade iteration was again scaled to a length of 22 in and printed in five sections, like the previous one. The print orientation was fixed, creating a smoother surface finish, and the issues with the mechanism were addressed. In addition to the blades, a hub was designed onto which the blades could be mounted, and inside of which the motor could be secured. Drawings of these models are found in Appendix B.

Standards

There are many standards that are relevant to the design and manufacture of wind turbines in the industry. Some of the code defining organizations involved in creating these standards include the International Electrotechnical Commission (IEC), the American Society of Testing and Materials (ASTM), the Underwriter's Laboratory, and the American Gear Manufacturers Association (AGMA) (Wilhite, 2020). There are three main categories of wind turbine standards: noise control, performance, and safety. In order to regulate the noise generated by wind turbines that has the potential to disrupt the sleep and cause headaches for people living nearby, IEC 61400-11 was instituted to standardize the methods for measuring the noise made by wind turbines. Also, while not specifically created for wind turbines, ASTM E1780-12, E1503-12, E1779, and E1014-12 include measuring methods and statistical test procedures for analyzing sounds produced by fixed sources which includes wind turbines (ANSI, n.d.). AGMA 10FTM13 includes requirements for gearboxes in wind turbines to reduce the noise levels (Wilhite, 2020). Performance standards for wind turbines include sections 1, 13, 21, 23, and 24 of IEC 61400 which includes design requirements, load and stress measurement methods, power quality assessment, structural testing, and lightning protection requirements respectively (ANSI, n.d.). AGMA 10FTM02 and 10FTM03 also include the improvement of the flexibility of heat treating wind turbine gears and ways to refurbish old gears in wind turbines (Wilhite, 2020). Finally, UL 6142 covers the safety of power generation systems in wind turbines regarding their connection to the electrical grid (Engineering 360, 2012). These are only some of the relevant standards, as available standards for offshore wind turbines are outside of the scope of this project. All of these standards must be taken into account when designing and building real-life wind turbines.

Risk Analysis

Concurrent with the development of the active control system, the team completed a Failure Modes and Effects Analysis (FMEA) of the control system components to identify and address potential failures of the system to ensure safe and reliable performance over the lifetime of the turbine. The FMEA was completed with a fully scaled turbine and system in mind to further demonstrate the upward scalability of the active control system. Hence, the spring-string mechanism was replaced by a hydraulic actuator system in the FMEA risk analysis.

The named components of the system were as follows: motor actuators, power controls, software, computer hardware, flap, and hydraulic actuator mechanism. Each component was carefully analyzed for failure modes, primarily mechanical and electrical failures, and a wide range of potential root causes were identified. The failure mode and root cause data are summarized in Appendix F-1. Next, each failure mode and cause were explored to assign an occurrence, severity, and detection score. These scores were used to determine the associated risk score of the failure mode. Two divisions of failure modes were identified: rare, but catastrophic, and common, but non-fatal. The first division (rare, but catastrophic) primarily affects the overall safety score of the wind turbine and is largely not a function of the active control system itself. For example, lightning striking the turbine would cause complete and catastrophic failure of the turbine, but is not a function of the active control system, rather the weatherability of the turbine itself. Therefore, the team focused on control system specific failures to determine the reliability risks of installing the active control system onto current turbine blades.

The analysis shows the most severe risk of the control system would be mechanical failure of the hydraulic actuator responsible for the extension and retraction of the trailing edge flap. Root causes of this failure mode include bolt shear from improper installation, gust events,

and inappropriate safety factors in design. It is encouraged for manufacturers to prioritize strength and safety over component weight of the actuator. High strength steel and high safety factors should be used in design. Often used in levee design, the hydraulic actuator should be able to easily withstand gusts characteristic of a 100-year storm event. Installation checks and testing should be standard to ensure no failures arise at the fault of the manufacturer.

Next, failure modes that pose a risk to critical electrical components in the control system were identified. As electrical failures often account for a large portion of non-fatal failures, extremely reliable electrical components are key to a high overall reliability of the control system. The team identified several root causes for electrical failure in the power, controls, and actuator mechatronic systems of the control system including particle contamination, excessive moisture, temperature, electrical overload events, and shorted circuits. To address these failure modes, seals should ensure waterproofing and filtration systems should catch particles before their entry to computer hardware and control component areas. Annual cleanings/maintenance testing should evaluate the health of electrical components of the active control system. Battery power backups and capacitors should be installed to handle fluctuations in power frequency, and emergency overrides should be in place in case of a power surge event to protect the integrity of the circuitry in the control system.

Finally, software issues present the least severe failures of the control system. These failure modes include improper data collection and storage, synchronization errors, and control system malfunctions. Most of these software issues can be addressed with thorough and complete testing, especially in edge and unlikely cases.

Solution

Final Design

The final turbine design was modeled in Solidworks as seen in Figure 14 below. The rotor consisted of 3 blades and a hub. Each of the blades contained a slot on the trailing edge for the extending flap, housing for up to 5 springs, and a path for the string to follow from the flap to the hub. To allow for incorporation of internal components and accommodate the size of the 3D printer being used, each blade was printed in halved segments. The hub consisted of an oblong outer structure and a frame to hold the motor in place. A small hole was placed in the front to place a slip ring. Another hole was placed in the back of the hub to provide a place to mount the rotor to a generator. The hub was also printed in halves so that the motor and electrical components could be incorporated into the system, as well as allowing for disassembly for maintenance of the components inside the hub.

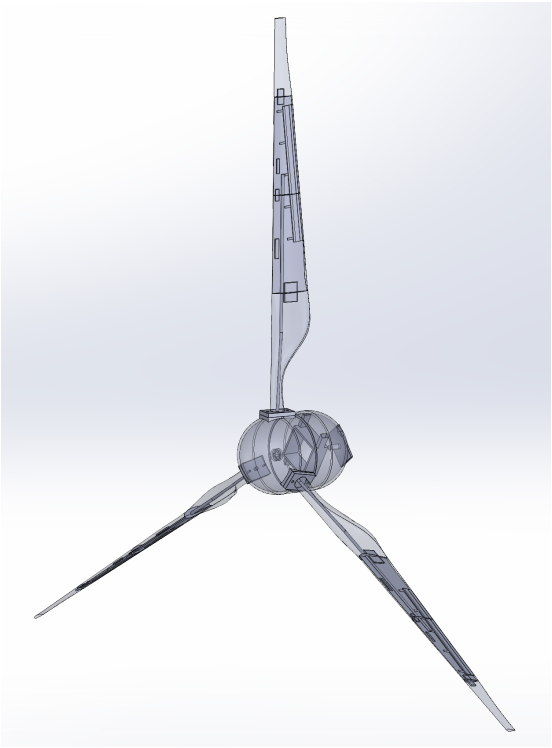

Figure 14: Final Solidworks Model of Wind Turbine Assembly

For the motor the team chose to use a bipolar stepper motor because of its ability to remember position and the superior holding torque compared to servo motors. To minimize the amount of weight in the turbine and keep the hub size small, the team found the smallest bipolar stepper motor with torque ratings appropriate to accommodate the force of the springs. The motor selected was the NEMA 17 Bipolar Stepper Motor which had a maximum current of 2A and a maximum holding torque of 59 N-cm. The motor was connected to an Arduino UNO Rev3 and Arduino Motor Shield Rev3. Instead of powering the motor through the Arduino, the motor was powered directly through the Motor Shield using a 9V battery. To control the motor, code was written that prompted a user for the wind speed input in the serial monitor of the connected computer (Appendix E). The code then checked the position of the motor and adjusted its position based on the corresponding flap position for that wind speed. The motor was to hold a spool for the string to wind around during operation. The radius of the spool was used to determine the number of stepper motor steps between each of the flap extension settings.

The strings were to travel down the internal channel designed in the blade and attach to the flaps in the slot on the trailing edge. Fishing wire was used as the chosen string due to its thinness and relatively high tensile strength which allows it to hold a significant amount of weight without snapping or deforming. Only two springs were placed in the blades of the final turbine due to the fact that only small, very specific springs could fit in the housing. Specifically, springs with a 0.088in outer diameter. These springs were difficult to find and expensive compared to the other purchased components.

Due to time constraints and difficulty constructing a turbine on such a small scale, the group was not able to actualize the planned active control system to control the movement of the flaps. The blades themselves were only an inch wide and approximately a quarter of an inch

thick, leaving very little room for error. Tolerancing the 3D printed pieces to such close values proved to be difficult and small tolerance changes during construction did not leave room for the flaps to freely move in the trailing edge of the blade. The original turbine design was maintained but the motor and spring pulley system was omitted from the turbine.

Experimental Setup

To test the original idea for the active control system without the intended mechanism, the team cut individual flaps of different lengths to emulate the different placements of the flap during extension and retraction. These flap lengths included 0.75, 1.00, 1.25, 1.50, 1.75, 2.00, 2.25, and 2.50 inches. The slots were a quarter of an inch deep, meaning the part of the flap extending out of the blade was a quarter inch less than the actual length of the flap. Each of these flap lengths were placed in the trailing edge slots and tested under various wind conditions. Trials were also run with no flap to provide a control for comparison. The wind tunnel speeds tested included 5, 10, 15, 20, 25, and 30 m/s, while the actual speeds experienced by the wind turbine were lower. These values are shown in Figures 16 and 17. Three trials were conducted at each wind speed. Due to the fact that the available wind tunnel had very limited testing space inside the tunnel, only one cubic foot, the turbine was placed behind the tunnel for testing. To account for pressure losses and a decrease in velocity behind the wind tunnel, multiple measurements of wind speeds were taken behind the wind tunnel using a handheld anemometer (Appendix C-1). The speeds entered into the tunnel control system were much higher than the speeds experienced behind the tunnel and varied on average by a factor of 3.372. These wind speeds are the ones featured on Figures 16 and 17. To measure how the flap length affected the power output of the turbine at different wind speeds, voltage measurements were taken using a digital multimeter (DMM). The DMM was hooked up to leads extending from the generator to

which the rotor was mounted to. A 12V DC gear motor was used as the generator, and this was attached to a wooden stand, shown in Figure 15 below.

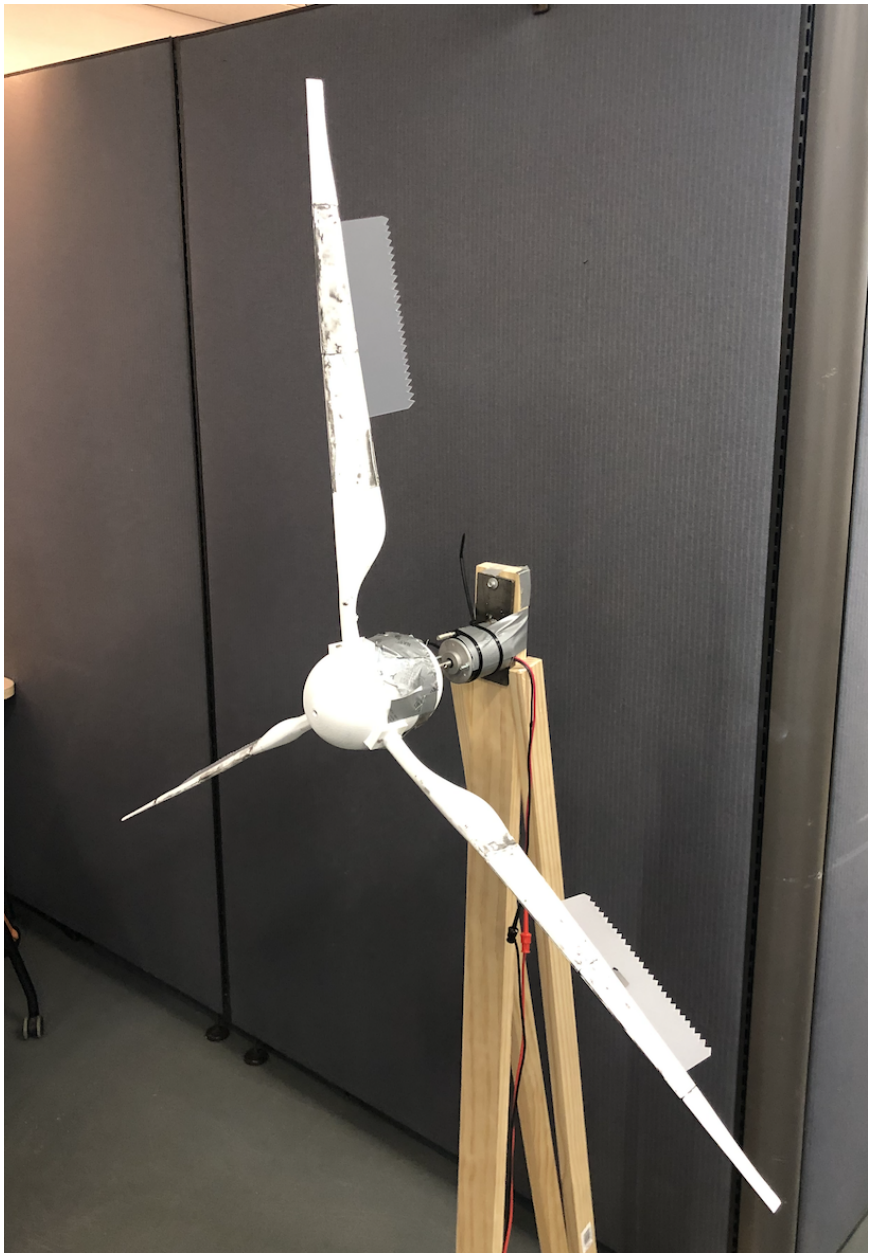

Figure 15: Turbine Setup for Wind Tunnel Testing

Test results for the unaltered flaps are seen in Figure 16 below. Full results are located in the table located in Appendix D. The graph shows the average voltage output at each wind speed for each flap length. As seen on the graph, most of the values are very close in range making it

hard to distinguish performance between the individual flap lengths. The results do clearly show that the control tests without a flap overall had lower voltage outputs than those with the flap. Less apparent is that the flap length that performed the best overall is 1.25 in, or 1 in extending from the blade, just as the simulation predicted. As flap length increased the voltage output was increasing up until 1.25 in. After this value the voltage output began to decrease slightly with flap length.

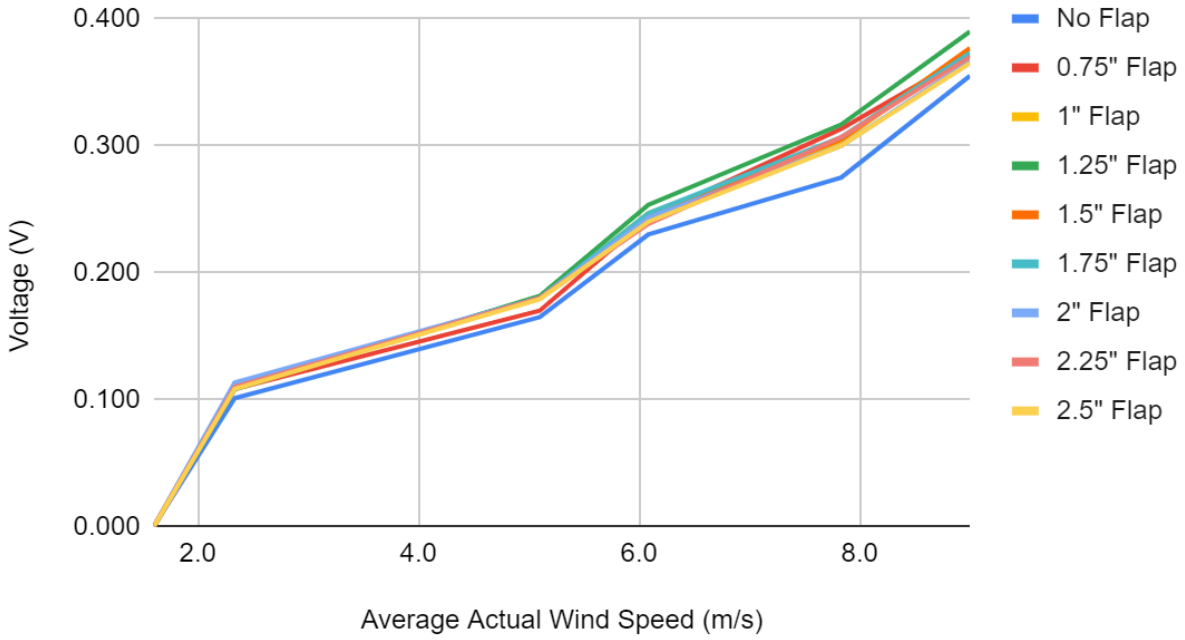

Figure 16: Voltage vs. Wind Speed Graph for Unaltered Flaps

Since the active control system did not ultimately make it to the testing phase of the project, the group decided to also alter the flaps for more data and to see if different shapes had any impact on their effectiveness. To alter the flaps, quarter inch serrations were cut into the trailing edge. The original tests were repeated for three trials of each flap length and wind speed. Similar to the unaltered flaps, the graphs of the individual serrated flaps overlap and are hard to distinguish from each other, seen in Figure 17. The result that blades with flaps produced more voltage output than the control trials remained consistent.

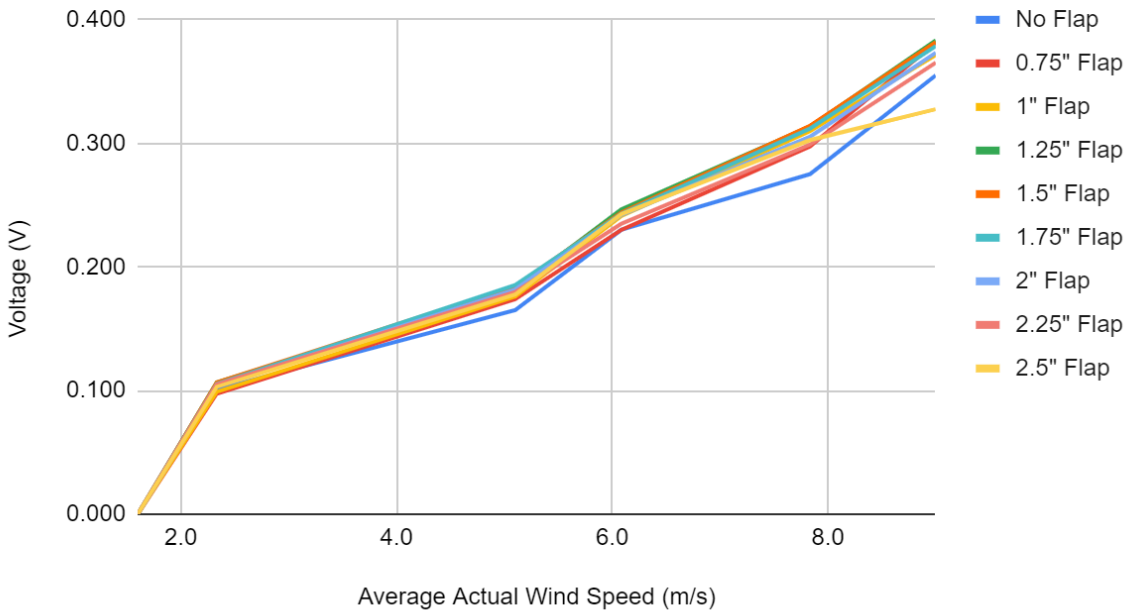

Figure 17: Voltage vs. Wind Speed Graph for Serrated Flaps

In addition to the lack of an active control system in the final turbine, there were other aspects that limited the scope of testing and could have affected the results. Because the turbine had to be placed behind the wind tunnel, there was a limit to the range of wind speeds that could be tested. Even with the tunnel operating at 30 m/s, the wind felt behind the tunnel was only at a speed of 9 m/s. This limited the results that could be found. Additionally one of the blades weighed less than the other two. During initial construction one of the string paths was blocked and holes were needed to unblock the passage. This imbalance of weight could have affected the turbine and its cut-in speed. If the experiment were repeated it would be better and more accurate to test in a larger wind tunnel and ensure that each blade had the same weight.

Public Safety and Environmental Considerations

With the introduction of any new form of technology, several factors must be brought into consideration to ensure the safe implementation of a new design into society. Therefore, public health and safety were a part of the group's decision making process before the start of the

experiment. Wind turbines are not especially dangerous to people, but do possess a large amount of noise pollution in areas where wind farms with many turbines are located, even having the potential of disrupting sleeping patterns of those living nearby (GE News, 2014). The addition of the new way to improve turbine efficiency will allow the blades to generate more power at lower speeds, which will reduce on average the amount of noise pollution created by the machines.

A more important aspect to consider is any impact that this project's proposed addition for wind turbines will have on global, social, cultural, or environmental (GSCE) factors. The possible economic impact of renewable energy is expected to bring an increase of 1.1% to the global GDP and create over 24 millions jobs by 2030 (IRENA, 2016). Therefore, it is crucial that research is conducted on the improvement of technology in the renewable energy sector to help improve the global economy. More important are the environmental factors in consideration. The increasing global concerns over climate change have caused more governments to look towards switching to renewable energy. With wind turbines being one of the leaders in the renewables industry, this project's main goal became to make advancements in the field in the hope that the transition away from fossil fuels will occur before climate change worsens.

While ultimately the goal of wind farm development is to mitigate the negative environmental impacts of fossil fuel-based energy generation methods, there are a few negative impacts that were not taken into consideration within the scope of this project. One of these is the impact that turbine operation has on the avian community. Wind turbines have been estimated to kill over 140,000 birds every year in just the United States (Hogan, 2020). This value is large but is relatively small compared to bird deaths caused by other man made structures like buildings and powerlines. Another issue that has been encountered is the disposal of turbine blades after their use. Wind turbines are being outfitted with new blades after 10 years, which is less than half

of their expected operating lifespan of 25 years (Martin, 2020). There are very few recycling programs in place for these blades so the majority of them are placed into landfills.

Cost Analysis

After completing the design of the active control system, a cost analysis was completed to ensure the viability of installing this active control system in a large scale wind turbine blade. Information regarding the bill of materials, cost of materials, estimated labor times, equipment, and capital costs are referenced from a 2019 NREL Wind Turbine Cost Model (Bortolotti, 2019). According to the model, made for a 130m rotor diameter, the overall cost per blade was $155,000. These figures were used as a baseline estimate for the current costs of manufacturing a turbine blade (Table 1).

Table 1: Cost Analysis for Manufacture of a Wind Turbine Blade

Category	**Cost Per Blade**	**Percent of Cost**
Materials	$73,600	47.5%
Labor	$49,800	32.1%
Utilities	$700	0.4%
Equipment	$15,400	9.9%
Building/Land	$700	0.4%
Maintenance	$4,400	2.8%
Capital	$8,700	5.6%

The mechanism covers one third of the chord length of the blade and travels along one third the length of the blade, adding an estimated one ninth of the surface area of the blade. An additional one ninth was added to the resin and composite material costs (Appendix G-2). Estimates were also made about the additional labor costs, which primarily affect the labor costs of the skin mold, assembly, and overlay of the blade due to the increasing geometric complexity. For the cost analysis, an additional 20% of labor costs was added to these categories. Estimates on bolt and cost for the hydraulic actuator proved difficult, primarily due to unavailable quoting for these systems for hobbyists. According to the NREL model, the cost of bolts and steel in a standard turbine blade is approximately $4,400 and it is estimated that the mechanism adds an additional $2,000 to this cost. These generous rates lead to an increase in material, labor, and manufacturing cost of $12,300 per blade, a 7.9% increase on the original $155,000. Visual representations of these statistics can be found in Appendix G.

The active control system requires additional motors, control, and power systems, with a generous estimate of $100,000 per turbine. Accurate estimates for these electronic components also proved difficult as models and prices are not easily found online and are often contractually determined between manufacturers.

In total, the additional estimated cost per turbine is $136,900 for the active control system. For a 2.5 MW turbine operating at 30% capacity, this would result in an increase in annual LCOE (Levelized Cost of Energy) of $0.021/kWh. The 10% increase in efficiency, and resulting capacity, more than balanced this cost out, bringing in an estimated $274,000/annum (based on 12.5 cents/kWh). The additional revenue generation was calculated according to the formula below.

$$Add.\ Revenue\ = (Rated\ Power\ Generation)\ *\ \Delta Capacity\ *\ \$/kWh\ *\ 8760h/yr \quad (5)$$

The cost of the control system is covered in 6 months of turbine operation, demonstrating the large added value of our system. It is important to note that these cost estimates do not include repair and maintenance costs, which would be better estimated through large scale testing of the mechanism.

Conclusion

The overarching goal of our project was to optimize power production between the cut-in and peak power production speeds of wind turbines. With methods such as active pitch control and increasing the swept area of turbines already in use, the team chose to explore varying the width of the blade as a potential improvement to current wind turbine design. Originally, the proposed solution aimed to actively change the width of each blade using a spring-string system driven by a stepper motor. However, the design of the active control system could not be adequately put together and tested due to the size constraints of the wind tunnel. The small-scale hub and blades left little tolerance for error in the design. Without this restraint, the final design could have been successfully tested on an appropriately larger-scaled turbine. In spite of the setback due to size constraints, the team moved forward and tested the 3-D printed turbine for voltage output at varying speeds with varying flap widths attached to the blades. Both flat and serrated trailing edge flaps were tested. Results showed that increasing the width of the blade with flaps, to any degree both flat and serrated, did increase the power production of the turbine compared to the power production of the turbine with no flaps.

While the results appear conclusive, the design of the experiment presents multiple sources of error as areas for improvement. As already mentioned, the limitations posed by size constraints did not allow for use of the test section of the wind tunnel. By testing the design at the outlet of the tunnel, the tunnel could not be tested at any desirable higher wind speeds than

those recorded. Additionally, air flow was not completely laminar past the outlet of the tunnel, which had an unquantifiable effect on any results. However, by running multiple trials, keeping the distance of the experimental setup from the tunnel constant, and recording wind speed averages with an anemometer, the team hoped to reduce any error from turbulence variations in all trials.

A great many opportunities exist for future work in the research and development of wind turbine efficiency and power production. With a clear increase in energy output due to the attachment of flexible flaps to the blades, further analysis accrediting these results to either the flap material or flap width would provide better insight into the aerodynamics of wind turbine blades. This insight could then make room for a clearly proven way of improving wind turbine power production. Additionally, further work could explore utilizing modular design to continue the sizing up of current wind turbines. Increasing turbine blade length increases their swept area, which has been proven to significantly improve energy efficiency. As the world begins to feel the initial effects of climate change, it is essential to continue research into wind turbine design and development as it may be crucial in the battle against global warming's most dire consequences.

References

Bortolotti, P., Berry, D. S., Murray, R., Gaertner, E., Jenne, D. S., Damiani, R. R., Barter, G. E., & Dykes, K. L. (2019). *A Detailed Wind Turbine Blade Cost Model*. http://www.osti.gov/servlets/purl/1529217/

Hamilton, T. (2008, March 6). *Whale-Inspired Wind Turbines*. MIT Technology Review. https://www.technologyreview.com/2008/03/06/221447/whale-inspired-wind-turbines/

Hogan, B. (2020, March 2). *Is it possible to build wildlife-friendly windfarms?* https://www.bbc.com/future/article/20200302-how-do-wind-farms-affect-bats-birds-and-other-wildlife

How Loud Is A Wind Turbine? (2014, August 2). GE News. https://www.ge.com/news/reports/how-loud-is-a-wind-turbine

How to control a Stepper Motor with Arduino Motor Shield Rev3. (n.d.). *Makerguides.Com*. https://www.makerguides.com/arduino-motor-shield-stepper-motor-tutorial/

How to input NUMBERS through Arduino serial.monitor. (2012, June). Arduino Forum. https://forum.arduino.cc/t/how-to-input-numbers-through-arduino-serial-monitor/107507/2

Martin, C. (2020, February 6). *Wind turbine blades can't be recycled, so they're piling up in landfills*. Los Angeles Times. https://www.latimes.com/business/story/2020-02-06/wind-turbine-blades

NACA 4421 (naca4421-il). (n.d.). http://airfoiltools.com/airfoil/details?airfoil=naca4421-il

Opie, R. (2018, March 2). *Pitch Control Critical for Wind Power*. Machine Design. https://www.machinedesign.com/mechanical-motion-systems/article/21836463/pitch-control-critical-for-wind-power

Renewable Energy Benefits: Measuring the Economics. (2016). *IRENA*, 92.

Renewables became the second-most prevalent U.S. electricity source in 2020—Today in Energy—U.S. Energy Information Administration (EIA). (2021, July 28). Eia. https://www.eia.gov/todayinenergy/detail.php?id=48896

Size evolution of wind turbines over time. (n.d.). ResearchGate. https://www.researchgate.net/figure/Size-evolution-of-wind-turbines-over-time_fig1_221911675

UL 6142—UL Standard for Safety Small Wind Turbine Systems. (2012, November 30). Engineering 360. https://standards.globalspec.com/std/14333165/UL%206142

U.S. Renewable Energy Factsheet. (2021). Michigan Center for Sustainable Systems. https://css.umich.edu/factsheets/us-renewable-energy-factsheet

Wilhite, T. (2020, July 8). *Wind Turbine Standards*. HubPages. https://discover.hubpages.com/technology/Wind-Turbine-Standards

Wind Turbine Standards. (n.d.). ANSI. https://webstore.ansi.org/industry/energy/wind-turbine

Appendix A
Screening and Selection

Selection Criteria	A (3 separate motors to change pitch)	B (motor with gears to change pitch)	C (extend blade width w/ hydraulic actuator)	D (extend blade width w/ rack and pinion)	E (piston to change pitch)	F (airplane flaps)
Constructability	-	-	-	-	-	-
Energy Use	-	-	-	-	-	-
Reliability (durability)	-	-	-	-	-	-
Size (scalability)	0	0	-	0	-	-
Weight	-	-	-	-	-	0
Energy Production	+	+	+	+	+	+
Precision Movement	+	+	-	+	+	+
Pluses	2	2	1	2	2	2
Sames	1	1	0	1	0	1
Minuses	4	4	6	4	5	4
Net	-2	-2	-5	-2	-3	-2
Rank	2	2	4	2	3	2
Continue?	yes	combine w/ I	no	yes	no	yes

Selection Criteria	G (serrated trailing edge to change blade shape)	H (blade extenders to change width of blade)	I (blade extenders to change length of blade)	J (Tubercles)	Reference (turbine with no pitch control)
Constructability	-	-	-	0	0
Energy Use	-	-	-	0	0
Reliability (durability)	-	-	-	0	0
Size (scalability)	+	-	-	0	0
Weight	+	0	0	-	0
Energy Production	+	+	+	+	0
Precision Movement	+	+	+	+	0
Pluses	4	2	2	2	N/a
Sames	0	1	1	4	N/a
Minuses	3	4	4	1	N/a
Net	1	-2	-2	1	N/a
Rank	1	2	2	1	N/a
Continue?	no	no	combine w/ B	no	

(A-1a and A-1b) Figure 18: Screening Matrix of Brainstormed Ideas

Scoring									
	Weight	A (3 separate motors to change pitch)		B/I (Motors and lead screw to extend blade length)		D (extend blade width w/ rack and pinion)		F (airplane flaps w/ motor)	
Selection Criteria		Rating	Weighted Score	Rating	Weighted Score	Rating	Weighted Score	Rating	Weighted Score
Constructability	0.15	4	0.6	2	0.3	3	0.45	2	0.3
Energy Use	0.1	2	0.2	3	0.3	3	0.3	3	0.3
Reliability (durability)	0.2	3	0.6	3	0.6	3	0.6	3	0.6
Size (scalability)	0.05	2	0.1	5	0.25	3	0.15	3	0.15
Weight	0.1	2	0.2	3	0.3	4	0.4	4	0.4
Energy Production	0.25	4	1	4	1	4	1	3	0.75
Precision Movement	0.15	5	0.75	4	0.6	4	0.6	4	0.6
	Total Score		3.45		3.35		3.5		3.1
	Rank		2		3		1		4
	Continue?	no		no		yes		no	

(A-2) Figure 19: Scoring Matrix of Proposed Solutions

Appendix B
Solidworks Design

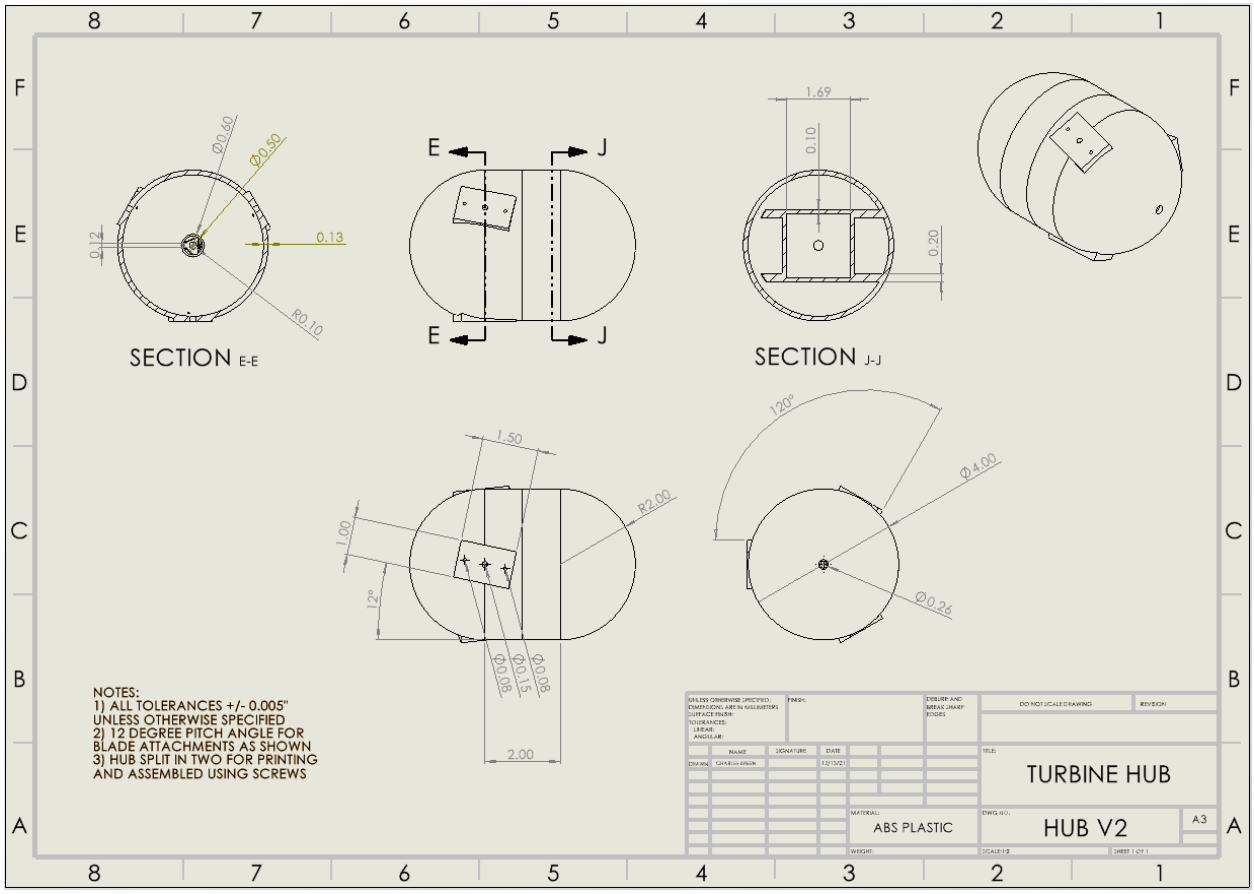

(B-1) Figure 20: Mechanical Drawing of the Turbine Hub (HUB V2)

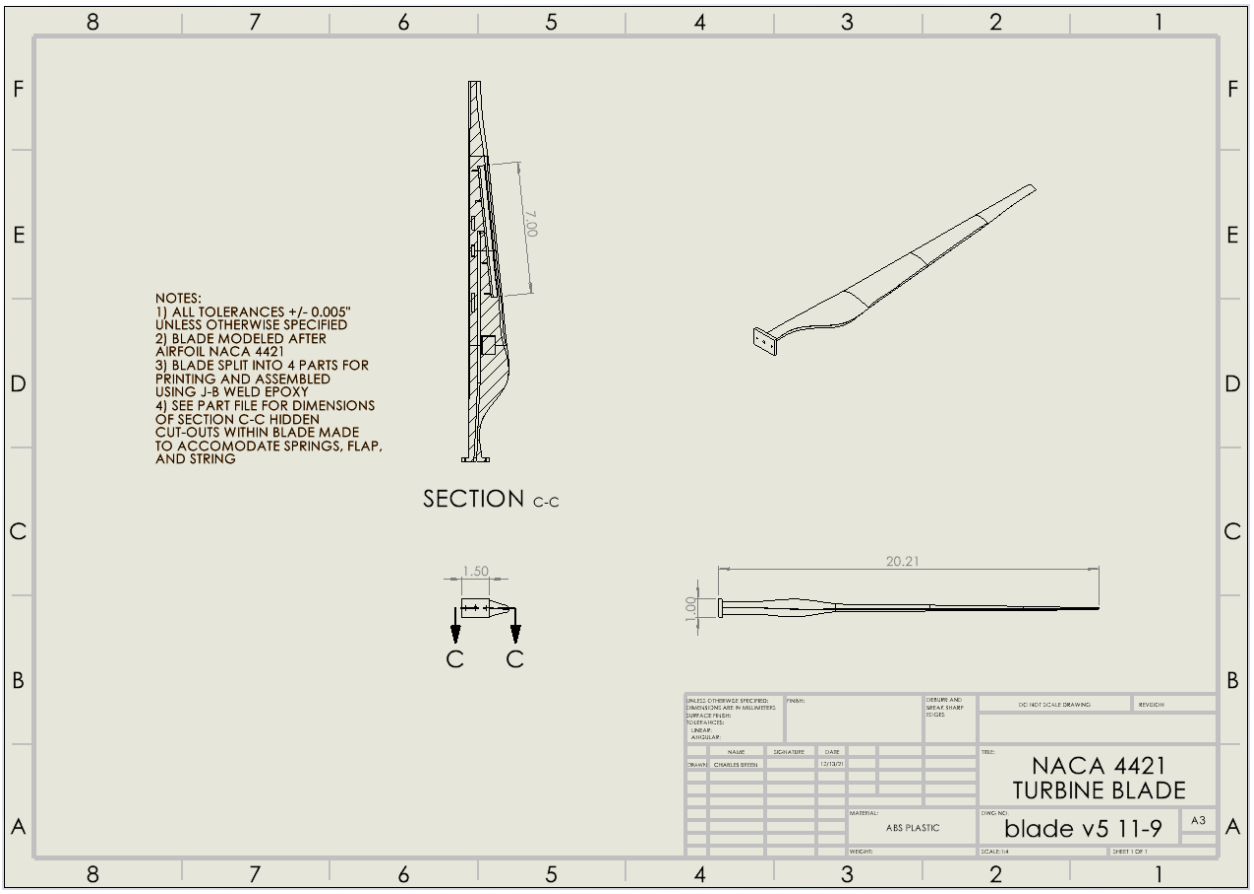

(B-2) Figure 21: Mechanical Drawing of Turbine Blade (blade v5 11-9)

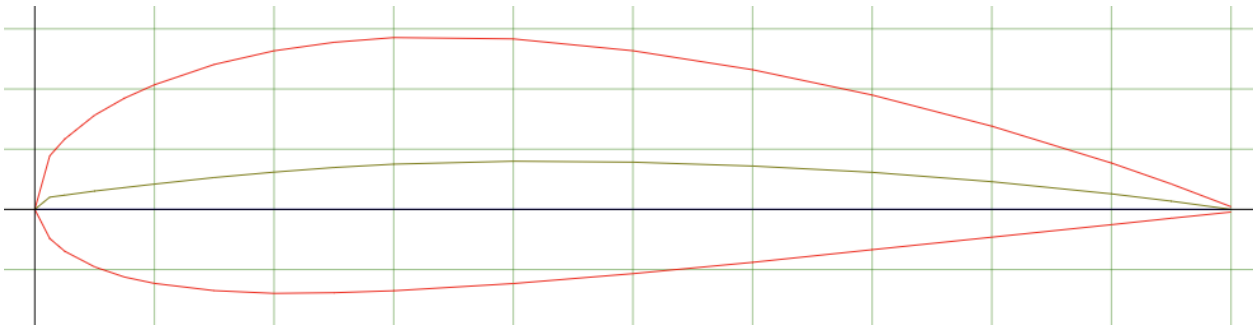

(B-3) Figure 22: NACA 4421 Airfoil (NACA 4421, n.d.)

Appendix C
Testing Constants

(C-1) Table 2: Anemometer Measurements Taken to Estimate Average Wind Speed Behind Wind Tunnel Given Input Wind Tunnel Speed

Input Wind Speed (m/s)	Actual Speed Trial 1 (m/s)	Actual Speed Trial 2 (m/s)	Actual Speed Trial 3 (m/s)	Actual Speed Trial 4 (m/s)	Actual Speed Trial 5 (m/s)	Actual Speed Trial 6 (m/s)	Avg. Actual Wind Speed (m/s)
5	1.2	1.8	1.8	1.6	1.6	1.6	1.6
10	1.7	2.5	2.5	2.4	2.3	2.6	2.3
15	5.0	5.0	5.0	5.6	5.0	5.0	5.1
20	6.0	6.0	6.5	6.0	6.0	6.0	6.1
25	8.0	8.0	8.0	8.0	8.0	7.0	7.8
30	9.0	9.0	9.0	9.0	9.0	9.0	9.0

(C-2) Table 3: Corresponding Lengths of Each Numbered Flap

Flap Length (in) Key	
F1	0
F2	0.75
F3	1
F4	1.25
F5	1.5
F6	1.75
F7	2
F8	2.25
F9	2.5

Appendix D
Testing Results

(D-1) Table 4: Testing Results for Unaltered Flaps

Run 1									
Avg. Actual Wind Speed (m/s)	No Flap (V)	Flap 2 (V)	Flap 3 (V)	Flap 4 (V)	Flap 5 (V)	Flap 6 (V)	Flap 7 (V)	Flap 8 (V)	Flap 9 (V)
1.6	0.000	0.000	0.000	0.000	0.000	0.000	0.000	0.000	0.000
2.3	0.098	0.105	0.110	0.112	0.110	0.115	0.115	0.115	0.105
5.1	0.160	0.165	0.180	0.185	0.180	0.180	0.180	0.180	0.180
6.1	0.230	0.250	0.250	0.250	0.250	0.250	0.245	0.235	0.240
7.8	0.275	0.320	0.310	0.320	0.310	0.315	0.295	0.310	0.300
9.0	0.370	0.360	0.375	0.390	0.380	0.375	0.370	0.370	0.360
Run 2									
Avg. Actual Wind Speed (m/s)	No Flap (V)	Flap 2 (V)	Flap 3 (V)	Flap 4 (V)	Flap 5 (V)	Flap 6 (V)	Flap 7 (V)	Flap 8 (V)	Flap 9 (V)
1.6	0.000	0.000	0.000	0.000	0.000	0.000	0.000	0.000	0.000
2.3	0.100	0.110	0.110	0.112	0.110	0.110	0.110	0.105	0.115
5.1	0.170	0.170	0.180	0.180	0.180	0.180	0.180	0.180	0.177
6.1	0.230	0.240	0.250	0.250	0.240	0.245	0.245	0.240	0.240
7.8	0.270	0.320	0.300	0.320	0.305	0.305	0.300	0.305	0.300
9.0	0.340	0.380	0.380	0.390	0.380	0.370	0.370	0.380	0.360
Run 3									
Avg. Actual Wind Speed (m/s)	No Flap (V)	Flap 2 (V)	Flap 3 (V)	Flap 4 (V)	Flap 5 (V)	Flap 6 (V)	Flap 7 (V)	Flap 8 (V)	Flap 9 (V)
1.6	0.000	0.000	0.000	0.000	0.000	0.000	0.000	0.000	0.000
2.3	0.105	0.110	0.110	0.100	0.110	0.110	0.115	0.110	0.105
5.1	0.165	0.175	0.180	0.180	0.180	0.180	0.180	0.180	0.180
6.1	0.230	0.240	0.240	0.260	0.245	0.245	0.240	0.240	0.240
7.8	0.280	0.300	0.300	0.310	0.300	0.300	0.305	0.305	0.300
9.0	0.355	0.375	0.375	0.390	0.370	0.375	0.360	0.360	0.375
Averages									
Avg. Actual Wind Speed (m/s)	No Flap	0.75" Flap	1" Flap	1.25" Flap	1.5" Flap	1.75" Flap	2" Flap	2.25" Flap	2" Flap
1.6	0.000	0.000	0.000	0.000	0.000	0.000	0.000	0.000	0.000
2.3	0.101	0.108	0.110	0.108	0.110	0.112	0.113	0.110	0.108
5.1	0.165	0.170	0.180	0.182	0.180	0.180	0.180	0.180	0.179
6.1	0.230	0.243	0.247	0.253	0.245	0.247	0.243	0.238	0.240
7.8	0.275	0.313	0.303	0.317	0.305	0.307	0.300	0.307	0.300
9.0	0.355	0.372	0.377	0.390	0.377	0.373	0.367	0.370	0.365

(D-2) Table 5: Testing Results for Serrated Flaps

Run 1									
Avg. Actual Wind Speed (m/s)	No Flap (V)	Flap 2 (V)	Flap 3 (V)	Flap 4 (V)	Flap 5 (V)	Flap 6 (V)	Flap 7 (V)	Flap 8 (V)	Flap 9 (V)
1.6		0.000	0.000	0.000	0.000	0.000	0.000	0.000	0.000
2.3		0.097	0.099	0.112	0.104	0.111	0.101	0.106	0.106
5.1		0.172	0.175	0.183	0.180	0.179	0.180	0.181	0.178
6.1		0.232	0.246	0.245	0.243	0.239	0.240	0.232	0.244
7.8		0.300	0.310	0.313	0.315	0.310	0.304	0.301	0.306
9.0		0.385	0.367	0.382	0.380	0.378	0.373	0.362	0.367
Run 2									
Avg. Actual Wind Speed (m/s)	No Flap (V)	Flap 2 (V)	Flap 3 (V)	Flap 4 (V)	Flap 5 (V)	Flap 6 (V)	Flap 7 (V)	Flap 8 (V)	Flap 9 (V)
1.6		0.000	0.000	0.000	0.000	0.000	0.000	0.000	0.000
2.3		0.098	0.101	0.108	0.107	0.103	0.106	0.103	0.101
5.1		0.176	0.175	0.179	0.191	0.189	0.183	0.178	0.178
6.1		0.228	0.240	0.248	0.242	0.244	0.241	0.235	0.244
7.8		0.295	0.309	0.314	0.313	0.311	0.305	0.295	0.300
9.0		0.378	0.368	0.386	0.382	0.374	0.372	0.364	0.238
Run 3									
Avg. Actual Wind Speed (m/s)	No Flap (V)	Flap 2 (V)	Flap 3 (V)	Flap 4 (V)	Flap 5 (V)	Flap 6 (V)	Flap 7 (V)	Flap 8 (V)	Flap 9 (V)
1.6		0.000	0.000	0.000	0.000	0.000	0.000	0.000	0.000
2.3		0.930	0.097	0.100	0.109	0.102	0.106	0.106	0.102
5.1		0.175	0.178	0.184	0.182	0.188	0.182	0.180	0.177
6.1		0.236	0.238	0.247	0.247	0.246	0.245	0.238	0.240
7.8		0.301	0.311	0.314	0.315	0.315	0.307	0.301	0.302
9.0		0.377	0.380	0.382	0.384	0.384	0.375	0.370	0.378
Averages									
Avg. Actual Wind Speed (m/s)	No Flap	0.75" Flap	1" Flap	1.25" Flap	1.5" Flap	1.75" Flap	2" Flap	2.25" Flap	2.5" Flap
1.6	0.000	0.000	0.000	0.000	0.000	0.000	0.000	0.000	0.000
2.3	0.101	0.098	0.099	0.107	0.107	0.105	0.104	0.105	0.103
5.1	0.165	0.174	0.176	0.182	0.184	0.185	0.182	0.180	0.178
6.1	0.230	0.230	0.241	0.247	0.244	0.243	0.242	0.235	0.243
7.8	0.275	0.298	0.310	0.314	0.314	0.312	0.305	0.299	0.303
9.0	0.355	0.382	0.372	0.383	0.382	0.379	0.373	0.365	0.328

Appendix E
Motor Code

```
// This code takes a user input in the serial monitor for wind
speed
// the motor checks its position and then moves to the
corresponding
// position for that wind speed


int ByteReceived;
String readString;

// Including the AccelStepper library:
#include <AccelStepper.h>
// Define number of steps per revolution:
const int stepsPerRevolution = 200;
// Name the motor control pins:
#define pwmA 3
#define pwmB 11
#define brakeA 9
#define brakeB 8
#define dirA 12
#define dirB 13
// Define the AccelStepper interface type:
#define MotorInterfaceType 2
// Create a new instance of the AccelStepper class:
AccelStepper stepper = AccelStepper(MotorInterfaceType, dirA,
dirB);


void setup()   /****** SETUP: RUNS ONCE ******/
{
  Serial.begin(9600);
  Serial.println("Input wind speed (mph)");
  Serial.println();
  // Set the PWM and brake pins so that the direction pins can be
used to control the motor:
  pinMode(pwmA, OUTPUT);
  pinMode(pwmB, OUTPUT);
  pinMode(brakeA, OUTPUT);
  pinMode(brakeB, OUTPUT);
  digitalWrite(pwmA, HIGH);
  digitalWrite(pwmB, HIGH);
  digitalWrite(brakeA, LOW);
  digitalWrite(brakeB, LOW);
  // Set the maximum steps per second:
  stepper.setMaxSpeed(600);
```

```
  // Set the original position of the flap to be fully extended
  // Flap needs to be reset after each time
  stepper.setCurrentPosition(30);
}

void loop() {
  while (Serial.available()) {
    char c = Serial.read();  //collects a single serial byte from
serial buffer
    readString += c; //makes the string readString
    delay(2);  //slow looping to allow buffer to fill with next
character
  }

  if (readString.length() >0) {
    Serial.println(readString);  //so you can see the captured
string
    int n = readString.toInt();  //convert readString into a
number

    // auto select appropriate value, copied from someone elses
code.
    if(n <= 10)
    {
      Serial.print("Wind speed: ");
      if (stepper.currentPosition() > 30) {
        while (stepper.currentPosition() != 30) {
          stepper.setSpeed(-100);
          stepper.runSpeed();

        }
      }
      else
      {
        while (stepper.currentPosition() != 30) {
          stepper.setSpeed(100);
          stepper.runSpeed();
        }
      }
    }
    else if(n <= 20 and n > 10)
    {
      Serial.print("Wind speed: ");
      if (stepper.currentPosition() > 20) {
        while (stepper.currentPosition() != 20) {
          stepper.setSpeed(-100);
          stepper.runSpeed();
        }
```

```
      }
      else
      {
        while (stepper.currentPosition() != 20) {
          stepper.setSpeed(100);
          stepper.runSpeed();
        }
      }
    }
    else if(n <= 30 and n > 20)
    {
      Serial.print("Wind speed: ");
      if (stepper.currentPosition() > 10) {
        while (stepper.currentPosition() != 10) {
          stepper.setSpeed(-100);
          stepper.runSpeed();
        }
      }
      else
      {
        while (stepper.currentPosition() != 10) {
          stepper.setSpeed(100);
          stepper.runSpeed();
        }
      }
    }
    // For all speeds above 30 mph (or whatever we set it to)
    else
    {
      Serial.print("Wind speed: ");
      while (stepper.currentPosition() != 0) {
         stepper.setSpeed(-100);
         stepper.runSpeed();
      }
    }
    readString=""; //empty for next input
  }
}
```

(“How to control a Stepper”), (“How to input”, 2012)

Appendix F
Wind Turbine FMEA

(F-1) Table 6: FMEA Analysis for Turbine with Hydraulic Actuator

Failure Mode	Cause	Effect	Occurrence	Severity (1-10)	Detection (1-10)	Proposed Solution
Software Bug	Incomplete Testing	Improper Functioning of Controls System, Data Storage, Connection with Elec Grid	Medium, 1 in 10,000	Medium, 4	High, 7	Thorough Beta Testing
Electrical Failure in Motor	Manufacturing Defect, Overload, Short Circuit	Consequential Failure of Forebar	Low, 1 in 100,000	Medium, 5	High, 8	Emergency Shut-off/Ground System and Alert
Electrical Failure in Power System	Manufacturing Defect, Overload, Short Circuit	Unsteady Connection with Elec Grid, all control systems fail	Low, 1 in 50,000	High, 7	High, 9	Emergency Shut-off/Ground System and Alert
Mechanical Failure in Motor	Over Torque, Gust Event	Consequential Failure of Forebar	Medium, 1 in 25,000	Medium, 4	High, 8	Choose motor with appropriate torques, braking system for gust events
Total Mechanical Failure in Hydraulic Actuator	Gust Event, Poor Design	Release of Flap	Low, 1 in 100,000	High, 10	High, 10	High Safety Factor in Design
Rotational Speed Exceeds Rating	High Wind Conditions, Failure of Pitch Control/Hydraulic Actuator	Potential Mechanical/Electrical Failure of Control Systems	Medium, 1 in 10,000	Medium, 6	High, 10	brake system
Improper Extension/ Retraction	Nonfatal Mechanical Failure in Hydraulic Actuator, Jam, Small Bolt Shear	Efficiency Decrease	Low, 1 in 25,000	Low, 2	Medium, 4	Good Safety Factor
Electric Overload Event	Lightning, Power Surge	Potential Electrical Failures	Low, 1 in 75,000	Medium, 6	High, 10	Emergency Shut-off/Ground System and Alert
Overheat	T > 130F	Potential Electrical	Low, 1 in	Medium,	High, 10	Emergency

Event		Failures	50,000	5		Shut-off/Ground System and Alert
Freeze	T < 20F	Potential Mechanical/Electrical Failure of Control Systems	High, 1 in 1,000	Medium, 5	High, 10	Thermal Insulation, Waterproofing, extensive thermal testing
Natural Frequency Oscillations	Poor Design, Wind Conditions, Lack of Dampening	Complete Structural Failure of Blades	Low, 1 in 100,000	High, 9	High, 8	Dampening System, Thorough Computer Analysis
Data Storage Failure	Software Malfunction, Network Connection Lost	Decreased Detection of Software/Electrical Failure	Medium, 1 in 10,000	Low, 2	Medium, 5	Ethernet, Backup Blackbox
Synchronization Error	Software Malfunction, Reset Event, Computer Hardware Failure	Proper Mechanical Function of Actuator, but Improper System Function, Decreased Efficiency	Medium, 1 in 10,000	Low, 3	High, 7	External Battery, Backup Power Supply
Bolt Shear	Gust Conditions, Improper Installation, Manufacturing Defect	Potential Mechanical/Structural Failures	Medium 1 in 10,000	Medium, 4	Medium, 4	Installation Check, Good Safety Factor
Particle Contamination Inside Control Panels	Dust, Wind, Animals	Potential Electrical Failures	Low, 1 in 100,000	Medium, 4	Low, 2	Annual Cleaning/ Maintenance
Erosion of Leading Edge	Wind, Rain	Decreased Efficiency	High, 1 in 2	Low, 1	High, 10	Material Science, Modular Design
Water Inside Control Panels	Rain, Storm Conditions	Potential Electrical Failures	Low, 1 in 100,000	Medium, 6	Medium, 4	Waterproofing Design, Maintenance of Seals

(F-2) Table 7: Ranking of Failure Modes for Turbine with Hydraulic Actuator

Ranking	Failure Mode
1	Total Mechanical Failure Hydraulic Actuator
2	Electrical Failure in Power System
3	Water Inside Control Panels
4	Natural Frequency Oscillations
5	Particle Contamination Inside Control Panels
6	Rotational Speed Exceeding Ratings

Appendix G
Cost Analysis for Wind Turbine Blade

(G-1) Table 8: Labor and Cycle Time of the IEA Land-Based Reference Wind Turbine Blade

Operation	Labor [hour]	Skin Mold Gating CT [hour]	Nongating CT [hour]
Material cutting	41.71	[-]	14.22
Root preform lp	10.74	[-]	7.10
Root preform hp	10.74	[-]	7.10
Infusion shear web number 1	69.30	[-]	10.02
Infusion shear web number 2	69.42	[-]	9.99
Infusion shear web number 3	28.15	[-]	5.86
Infusion spar cap lp	59.75	[-]	9.07
Infusion spar cap hp	58.83	[-]	8.98
Lp skin	197.91	15.41	[-]
Hp skin	191.14	[-]	15.41
Assembly	186.23	6.60	[-]
Demolding	4.70	1.99	[-]
Trim	15.60	[-]	3.10
Overlay	53.14	[-]	6.52
Postcure	1.71	[-]	9.68
Root cut and drill	9.09	[-]	4.37
Root hardware installation	6.06	[-]	2.85
Surface preparation	68.38	[-]	8.67
Painting	23.14	[-]	5.87
Surface finishing	13.94	[-]	4.70
Weight balance	6.24	[-]	2.94
Final inspection	2.71	[-]	1.09
Shipping preparation	5.42	[-]	2.43
Total	**1,134.05**	**24.00**	**139.98**

(G-2) Table 9: Total Composite, Core, and Coating Costs IEA Land-Based Reference Wind Turbine Blade

Composites and filler	Cost with waste [$]	Resin and adhesive	Cost with waste [$]	Other parts	Cost [$]	
Bx GF	960.07	Resin	10,962.87	Bolts	1,361.36	
UD GF	9,414.32	Hardener	3,288.86	Barrel nuts	653.45	
Tx GF	13,783.83	Adhesive Part A	5,010.74	LPS	2,624.00	
Balsa	17,090.18	Adhesive Part B	926.99	Consumables	7,562.14	
						Total
Total	41,248.41	Total	20,189.46	Total	12,200.95	**73,638.82**

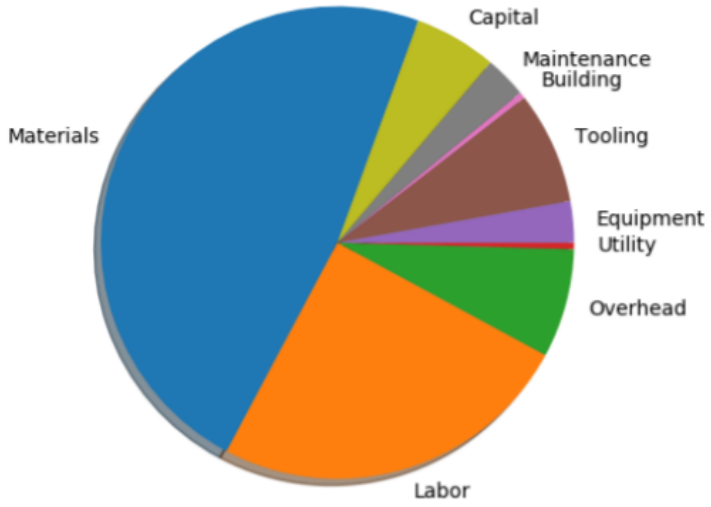

(G-3) Figure 23: Shares of the Overall Costs of the IEA Land-Based Reference Wind Turbine Blade

Appendix H
Project Expenses

(H-1) Table 10: Project Component Costs

Purchase	Cost/Unit	Quantity	Total Cost
3D Print Control Turbine	$23.00	1	$23.00
Slip Ring	$26.51	1	$26.51
Servo	$15.47	1	$15.47
Arduino Motor Shield	$21.95	1	$21.95
Arduino (+shipping)	$24.48	1	$24.48
m-f wires	$6.98	1	$6.98
Arduino USB Cable	$6.99	1	$6.99
Arduino Power Cable	$9.50	1	$9.50
22 Gauge wire	$12.98	1	$12.98
9V Battery Connector	$5.99	1	$5.99
9V Batteries (x4)	$13.99	1	$13.99
Blade Printing	$20	2	$40
First Total Print	$111	1	$111
Stepper Motor+fishing wire	$23.14	1	$23.14
Anemometer	$27.99	1	$27.99
Longer Springs (x8 +ship)	$79.56	1	$79.56
Amazon slip ring	$15.46	1	$15.46
Blade extension material	$14.73	1	$14.73
Small springs	$61.96	1	$61.96
		Total Spending	$541.68

Appendix I
Group Roles

Figure 24 shows the different groups that the team was broken down into and their general role descriptions.

Team	Member 1:	Member 2:	Member 3:
Mechanism Team	Amanda	Jason	Charlie
Description:	*Responsible for designing and prototyping a mechanism that extends the blades' width.*		
Design, Manufacturing, and Testing	Isaiah	Scott	Charlie
Description:	*Responsible for determining parts needed for design and testing of mechanism and performing peliminary calculations.*		
Operations Team	Amanda	Isaiah	
Description:	*Responsible for high level organization, keeping group on critical path, making sure timelines are met, and holding group meetings.*		
Validation Team	Scott	Isaiah	Astrid
Description:	*Responsible for FEA/CFD validation of ideas and preliminary testing of designs.*		
Documetation Team	Jason	Astrid	
Description:	*Responsible for keeping track of group finances and documents and organizing the final technical report.*		

(I-1) Figure 24: Division of Labor and Team Roles

Report Roles:

Jason Badu: Introduction, Background, Public/Environmental Consideration, Lead Editor

Charles Breen: Conclusion, Solidworks Drawings

Astrid Henkle: Final Design, Experimental Setup, Concept Drawings

Amanda Kassebaum: Concept Selection, Standards, Editing

Scott Morrow: Design Process, Decision Making

Isaiah Woo: Risk Analysis, Cost Analysis